

## **Chapter 6**

### **ESTIMATING ELECTRICAL AND THERMAL CONDUCTIVITY OF INTERPHASE**

---

#### **6.1 INTRODUCTION**

Under the influence of applied electrical stress, heat is generated in dielectric materials due to different kinds of losses. In a high voltage direct current (HVDC) system, conduction loss is the primary source of heat generation within the dielectric materials and conduction-based heat transfer is governed by the thermal conductivity of the dielectric material. Due to the fact that electrical conduction losses serve as a source of heat, thermal analysis under electrical (dc) stress requires prior knowledge of dc conductivity. Nanofiller inclusions are believed to affect both electrical and thermal conductivity. It has been demonstrated in previous investigations that the filler matrix interaction results in a third phase referred to as interphase. Prior information of the dc conductivity and thermal conductivity of the interphase is required to determine (numerically) the effectiveness of nanocomposites in increasing heat transfer capacity. In the preceding chapter, the size and permittivity of the interphase were estimated. This chapter applies the insight gained from the previous chapter to estimate the interphase's dc conductivity. Following that, quantified data on dc conductivity and interphase size are utilized to estimate the thermal conductivity of interphase in epoxy alumina nanocomposites.

## 6.2 ESTIMATION OF DC CONDUCTIVITY OF INTERPHASE

### 6.2.1 Methodology

The dc conductivity of interphase is estimated using a numerical model and experimental data in tandem. The first dc conductivity of base resin and nanocomposites is measured using an experimental procedure described in section 3.2.2, and the results are shown in Table 4.3. Following that, a numerical model is developed to estimate the effective dc conductivity of nanocomposites for known dc conductivity values of filler and base material. Because the DC conductivity of interphase is unknown, the numerical computation is started with some guess values. Subsequently, an iterative procedure elaborated in section 5.4 is used to assign a unique dc conductivity value to interphase. The effective dc conductivity of nanocomposites is estimated using finite element analysis (FEA). Various stages of FEA are depicted in Figure 6.1 and are described in detail in the following subsection.

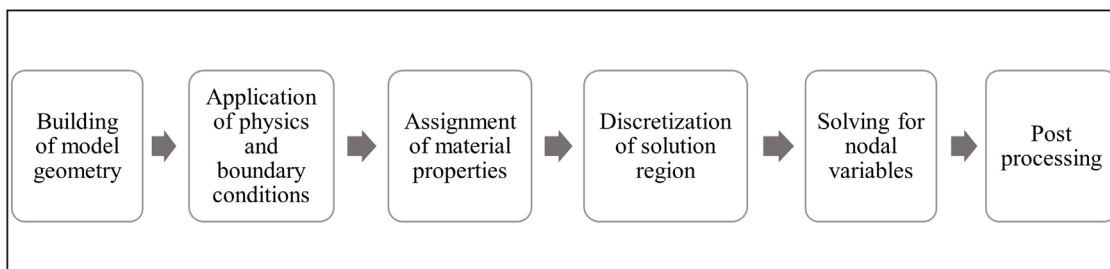


Figure 6.1 Flow diagram for performing finite element analysis

#### 6.2.1.1 Building of model geometry

Finite element analysis is carried out on a cubic unit cell with a size of  $1\mu\text{m}$  that contains randomly scattered nanoparticles. To simulate a 1 vol. percent filler concentration, the cubic unit cell illustrated in Figure 6.2 was incorporated with 153 nanoparticles each measuring 50 nm in diameter. Each nanoparticle is encapsulated in a

known-thickness interphase layer. In order to achieve random filler dispersion, java coding is used in the application builder tool of COMSOL Multiphysics. Furthermore, constraints are imposed on the center coordinates of nanofillers so that all nanoparticles are contained within the cubical block without overlap. A flow chart depicting the geometry building procedure is shown in Figure 6.3.

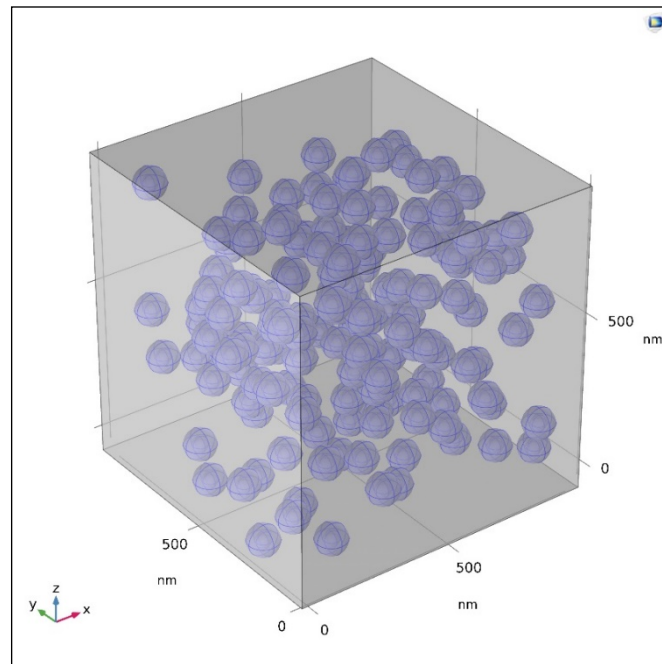


Figure 6.2 Randomly distributed multi-particle model

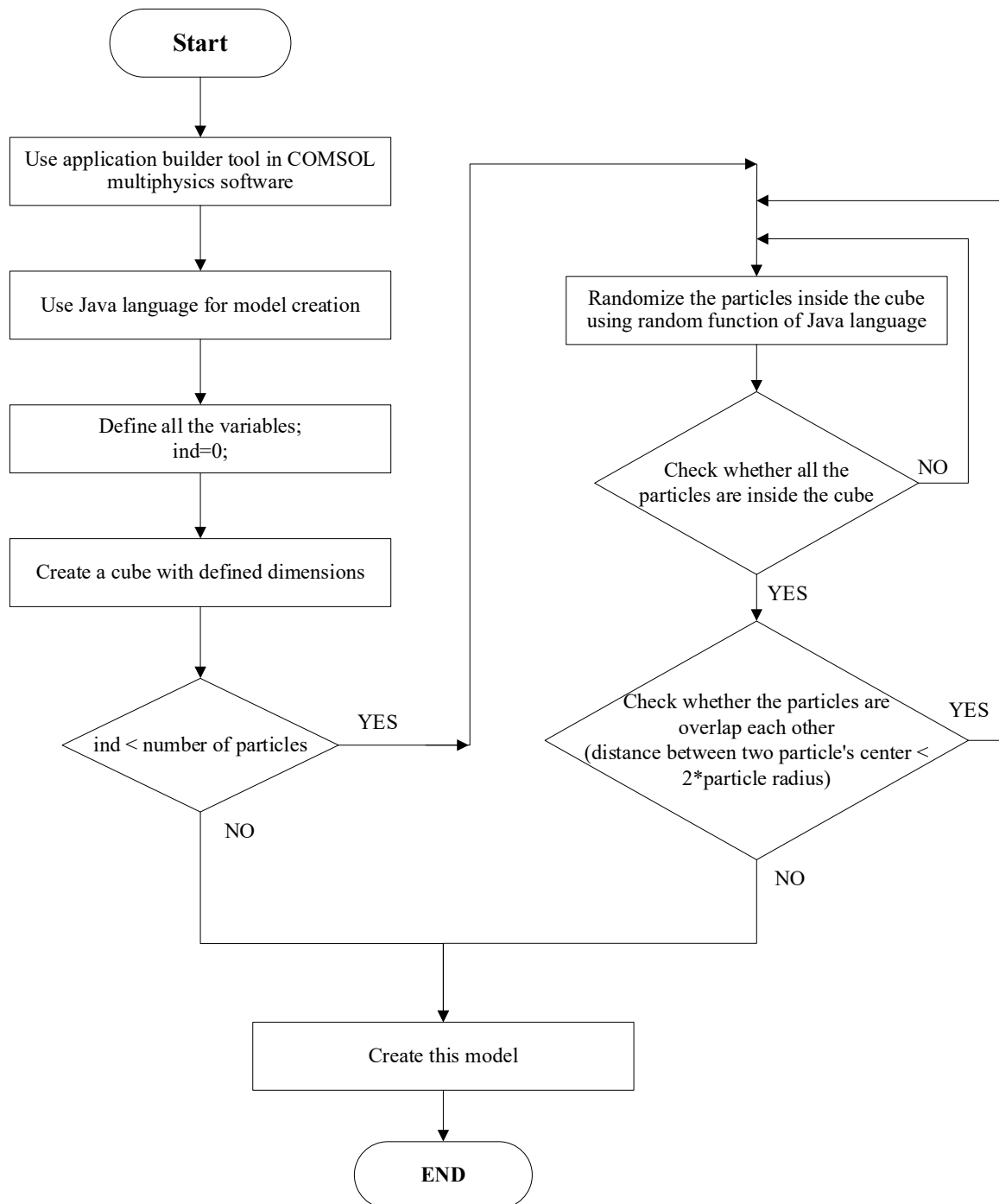


Figure 6.3 Flowchart to illustrate building of model geometry

### 6.2.1.2 Assignment of physics and boundary conditions

To perform numerical analysis, Electric Currents (ec) with AC/DC module of the COMSOL multi-physics software is used. Dirichlet boundary conditions were applied to the cube's front and back faces (i.e., 2V and 0V is specified respectively on the front and back faces). The remaining cube faces are subjected to the Neumann boundary condition (i.e.,  $\nabla \cdot D = 0$ ). Electric currents (ec) physics solves the Poisson equation and the continuity equation given below to compute nodal variables:

$$\nabla \cdot J = 0 \quad (6.1)$$

$$J = \sigma E \quad (6.2)$$

$$E = -\nabla V \quad (6.3)$$

Where

$J$  – Current density (A/m<sup>2</sup>)

$\sigma$  – Electrical conductivity (S/m)

$E$  – Electric field (V/m)

$V$  – Electric potential (V)

### 6.2.1.3 Assignment of material properties

The cubical block is assigned the material properties of epoxy resin (dc conductivity = 1.98E-14 S/m and relative permittivity = 4). Filler is assigned material properties of alumina (dc conductivity = 1E-12 S/m and relative permittivity = 10).

### 6.2.1.4 Calculation of effective electrical conductivity (dc) of the model

The effective dc conductivity of the composites is computed using the following equation:

$$\sigma = \frac{\langle J \rangle}{\langle E \rangle} \quad (6.4)$$

where  $\langle J \rangle$  and  $\langle E \rangle$  represent average current density and average electric field intensity respectively within the nanodielectric. A typical plot for potential, electrical field, and current distribution within the dielectric material is shown in Figure 6.4.

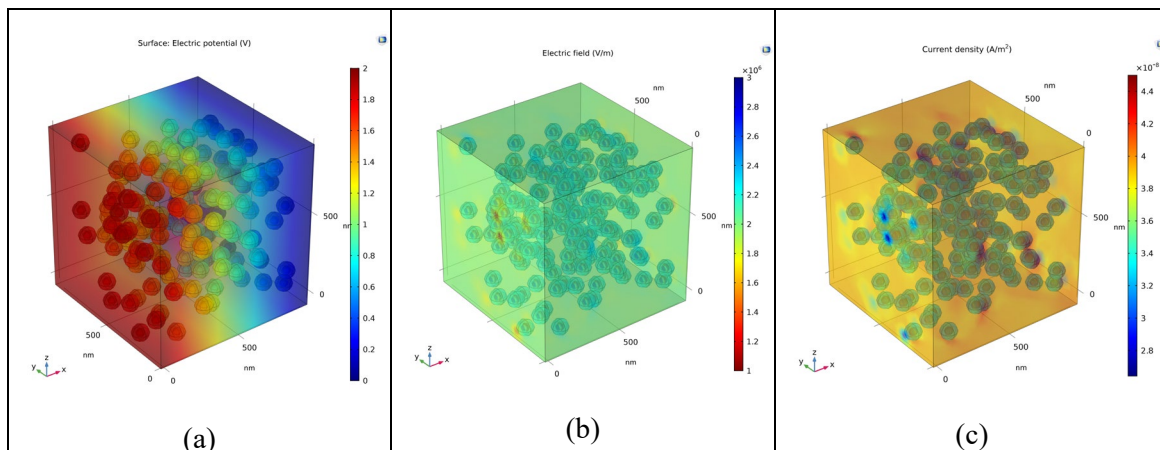


Figure 6.4 Potential, electric field and current density distribution with the nanodielectrics

### 6.2.1.5 Estimation of dc conductivity of interphase

Bisection method-based algorithm described in section 5.4 is used to estimate dc conductivity of interphase. Steps to implement the proposed algorithm are listed below:

Step 1-Record experimental dc conductivity values for pure epoxy and nanocomposites.

Step 2-Import the model created in COMSOL Multiphysics. Assign material properties, describe the model's physics, and apply appropriate boundary conditions.

Step 3-Set the electrical conductivity of nanocomposite to zero as an initial guess value. Specify a convergence tolerance value of 0.001. Assign a value of 0 as the initial mean, a value of  $1E-12$  as the upbound, and a value of 0 as the low bound.

Step 4-Compare measured electrical conductivity of nanocomposites to that computed using a numerical model. If this difference is more than the convergence tolerance limit, go to the next step. If the difference is less than the convergence tolerance, store the interphase's electrical conductivity value and exit the program.

Step 5-Calculate the mean value of upbound and low bound. Assign this mean value to interphase electrical conductivity.

Step 6-Calculate the current density and electric field using the numerical model. Determine the electrical conductivity of nanocomposite using current density value and electric field value. This nanocomposite electrical conductivity value should be stored.

Step 7-The computed value of the effective electrical conductivity of the nanocomposites is compared to the measured value. If the computed value exceeds the measured value, then assign upbound as the mean value. If the computed value is lower than the measured value, then a low bound is used as the mean.

Step 8-Return to step 4 and repeat until convergence is achieved.

To add in comprehension, this proposed algorithm is also represented using the flow chart shown in Figure 6.5.

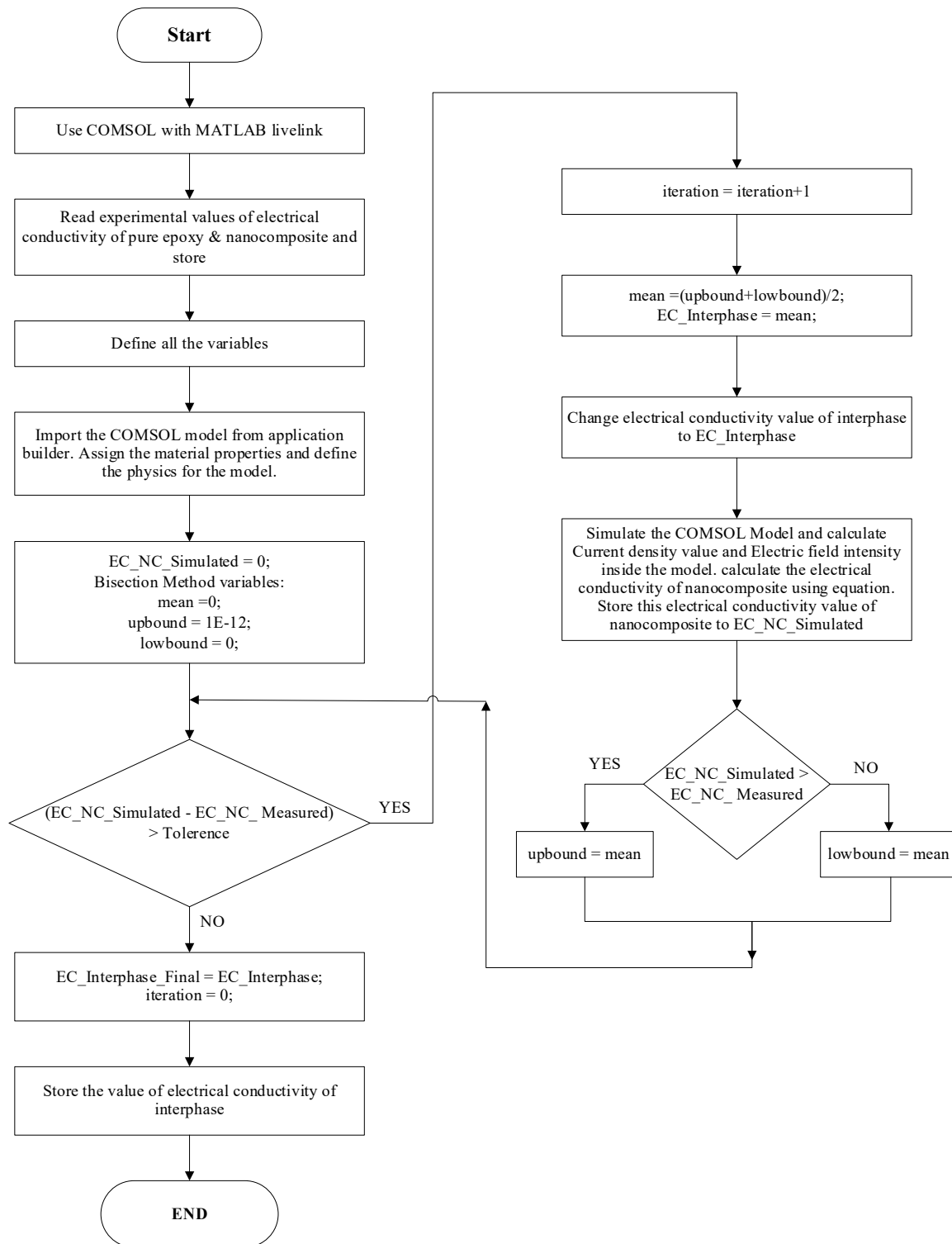


Figure 6.5 Flowchart to estimate the dc conductivity of the interphase

According to the proposed algorithm, the interphase dc conductivity is  $0.964\text{E-}14$  S/m.

This value is lower than the dc conductivity of the epoxy matrix. It implies that



interphase is crucial in lowering the electrical conductivity of nanocomposites. The structural changes around nanofillers have a significant impact on charge transport and conduction mechanisms, affecting the total conductivity of the nanocomposites.

## **6.3 ESTIMATION OF THERMAL CONDUCTIVITY OF INTERPHASE**

### **6.3.1 Methodology**

Interphase thermal conductivity is determined using a combination of experimental data and a computational model. To begin, the thermal conductivity of both the base polymer and the nanocomposite sample is measured. Following that, a numerical model is developed to predict the effective thermal conductivity of nanocomposites using known thermal conductivity values for the base polymer and filler material, as well as various assumed thermal conductivity values for the interphase. The algorithm described in Section 5.4 is used to assign a unique thermal conductivity value to interphase based on the best match between observed and numerically predicted effective thermal conductivity values for nanocomposites. The following subsection details the technique for measuring thermal conductivity and numerical modeling using finite element analysis.

#### **6.3.1.1 Thermal conductivity measurement**

The following specimens were synthesized for this study:

1. Pure epoxy samples
2. Nanocomposites samples (with nano alumina concentrations of 1 and 2 vol.%).

These samples were prepared using the procedure as described in chapter 3. Cubic samples of 15×15×15 mm in size were prepared to satisfy the instrument's (TPS 500) dimensional specification. Typical images of synthesized epoxy and nanocomposite samples (with filler content of 1 vol.%) are shown in Figure 6.6.

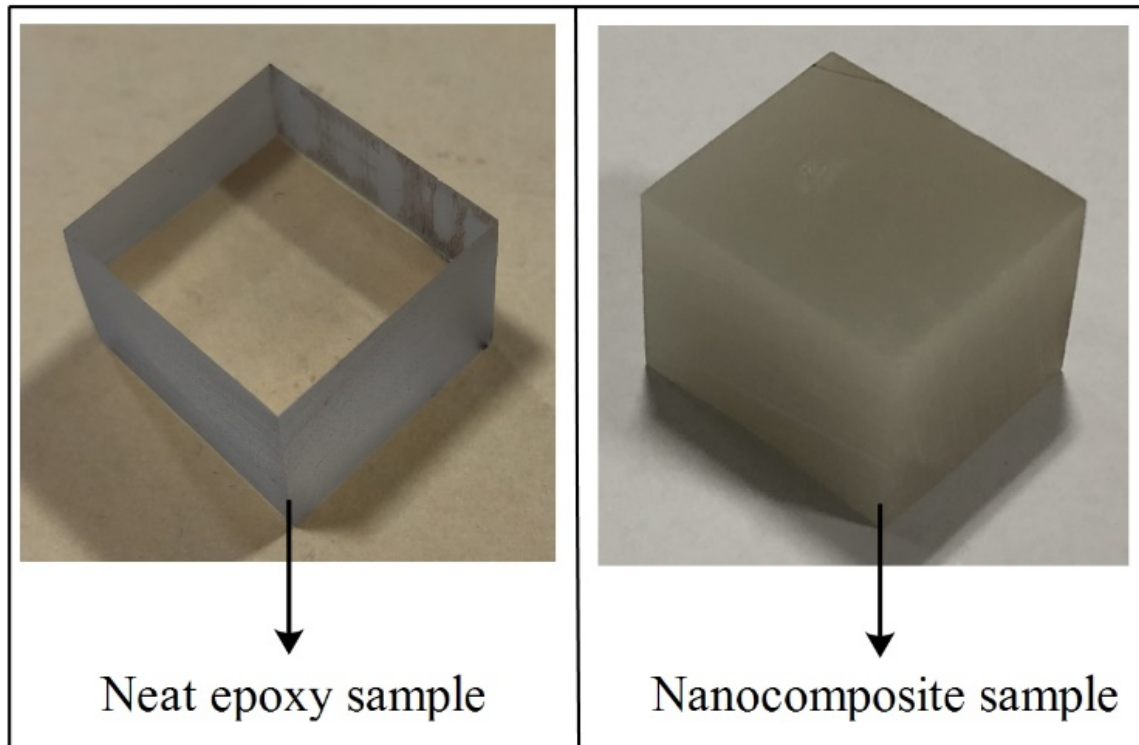


Figure 6.6 Neat epoxy and nanocomposite samples for thermal conductivity measurement

Thermal conductivity measurements were performed using a TPS 500 instrument shown in Figure 6.7. All measurements were performed following the standard test procedure recommended by ISO 22007-2:2008.



Figure 6.7 TPS 500 instrument in mechanical engineering department IIT (BHU)

Thermal conductivity measurements are performed by fitting the TPS sensor in between two pieces of a sample, as shown in Figure 6.8. To meet the requirement of thermal conductivity measuring setup, cubic samples with dimensions of  $15 \times 15 \times 15$  mm are chosen. Thermal conductivity was measured on five randomly selected samples from each specimen. A representative value (i.e., an average of five measurements) is shown in Table 6.1.

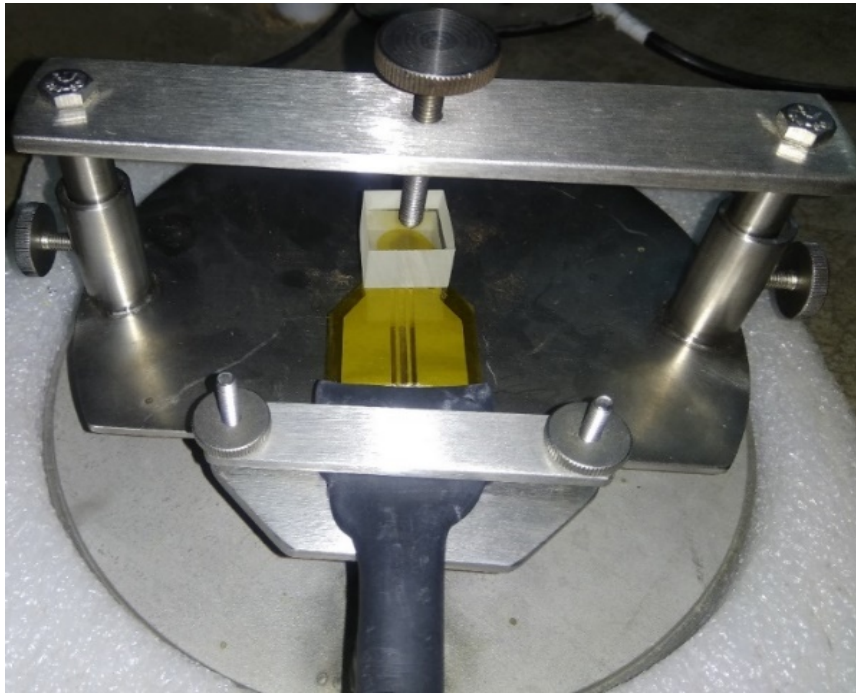


Figure 6.8 TPS sensor sandwiched between samples.

Table 6.1 Experimental values of thermal conductivity of specimens

Specimen	Thermal conductivity (W/K.m)
Neat epoxy sample	$0.160 \pm 1\%$
Nanocomposites sample (with filler content of 1 vol.%)	$0.174 \pm 1\%$
Nanocomposites sample (with filler content of 2 vol.%)	$0.192 \pm 1\%$

### 6.3.1.2 Numerical Modeling

#### 6.3.1.2.1 Building of model geometry

The model geometry is constructed in line with the technique described in section 6.2.1.1 and illustrated in Figure 6.3 with a flowchart.

### 6.3.1.2.2 Assignment of physics and boundary conditions

Joule heating module of COMSOL multi-physics software is used for this simulation study. Joule heating module involves electric currents (ec) and heat transfer in solids (ht) physics. Electric currents physics solves equations 6.1, 6.2, 6.3 described in section 6.2.1.2. Heat transfer in solids physics solves the following set of equations:

$$\nabla \cdot q = Q \quad (6.5)$$

$$q = -k\nabla T \quad (6.6)$$

Where,

$q$  – Heat flux ( $\text{W}/\text{m}^2$ )

$Q$  – Heat source ( $\text{W}/\text{m}^3$ )

$k$  – Thermal conductivity ( $\text{W}/\text{m}\cdot\text{K}$ )

$T$  – Temperature (K)

Boundary conditions specified in section 6.2.1.2 are used to estimate conduction losses. These conduction losses act as a heat source in thermal model. Dirichlet boundary conditions is applied on all outer boundaries of the cubic unit cell (i.e., a temperature of  $293^\circ \text{K}$  is specified on all outer boundaries of the model).

### 6.3.1.2.3 Assignment of material properties

Table 6.2 lists the material attributes that have been ascribed to each constituent phase. The density and heat capacity of the interphase material are considered to be the same as the matrix material in this study. Because the interphase thermal conductivity is unknown, the effective thermal conductivity of nanocomposites is calculated for various interphase thermal conductivity values obtained from an iterative technique described in later sections.

Table 6.2 Material properties of different constituents in the numerical model

Material properties	Epoxy	Alumina nanoparticles	Interphase
Thermal conductivity	0.16 W/K.m	30 W/K.m	-
Density	1.17 g/cm <sup>3</sup>	3.97 g/cm <sup>3</sup>	1.17 g/cm <sup>3</sup>
Heat capacity	1050 J/kg.K	880 J/kg.K	1050 J/kg.K
Electrical conductivity (dc)	1.98×10 <sup>-14</sup> S/m	1×10 <sup>-12</sup> S/m	0.964×10 <sup>-14</sup> S/m

#### 6.3.1.2.4 Calculation of effective thermal conductivity of the model

The effective thermal conductivity of composites is estimated using equation shown below:

$$\langle q \rangle = k \cdot \langle TG \rangle \quad (6.7)$$

Where  $\langle q \rangle$  represents the average heat flux magnitude over the volume of the cube,  $k$  denotes the effective thermal conductivity, and  $\langle TG \rangle$  represents temperature gradient.

#### 6.3.1.2.5 Validation of the Modeling Method

It is critical to ensure that the modelling technique described above in terms of physics and boundary conditions results in a solution with an acceptable accuracy limit. A simple geometry for which an analytical solution is possible is considered to verify the FEA described above. A spherical particle with a diameter of 50 nm is surrounded by a cube with a side length of 200 nm in the geometrical model depicted in Figure 6.9. The identical physics and boundary conditions stated in Section 6.3.1.2 are used in the finite element analysis. The thermal conductivities of the cube (host material) and the

spherical particle (filler) are 5 W/Km and 10 W/Km, respectively. Finite element analysis estimates an effective thermal conductivity of 5.031 W/K.m for this numerical model.

The next step is to establish an analytical solution [103] to validate the numerically predicted thermal conductivity.

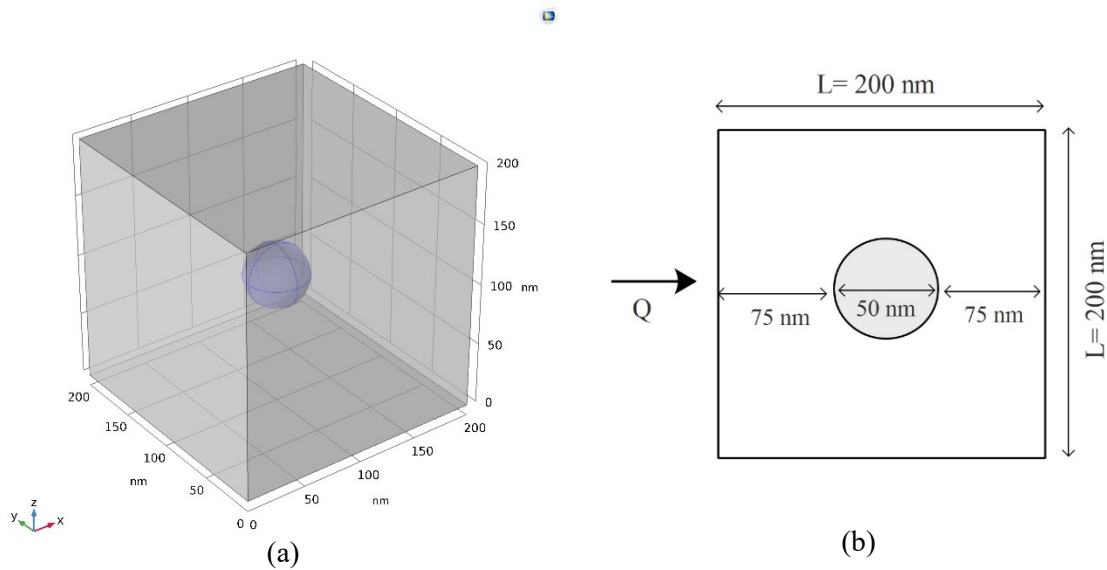


Figure 6.9 Model geometry considered for FEA and analytical study (a) 3-D view (b) 2-D view

Heat flow and thermal conductivity are related as per Fourier law [104] given below:

$$Q = kA \frac{\Delta T}{dx} \quad (6.8)$$

Where,

Q - Quantity of heat flow through the model (W)

k - Thermal conductivity (W/K.m)

A - Cross section area (perpendicular to the path of heat flow)

T - Temperature (K)

Equation 6.8 can be written as:

$$k = \frac{Q}{A\left(\frac{\Delta T}{dx}\right)} \quad (6.9)$$

Heat flows through three series-connected regions, A, B, and C, as shown in Figure 6.10. Thermal conductivities A, B, and C are denoted by the symbols  $k_A$ ,  $k_B$ , and  $k_C$ . Because A and B are the same material, their thermal conductivities are the same (i.e.,  $k_A = k_C$ ). Part B is made up of two materials (host and filler). The effective thermal conductivity value of part B ( $k_B$ ) is calculated using the procedure detailed below.

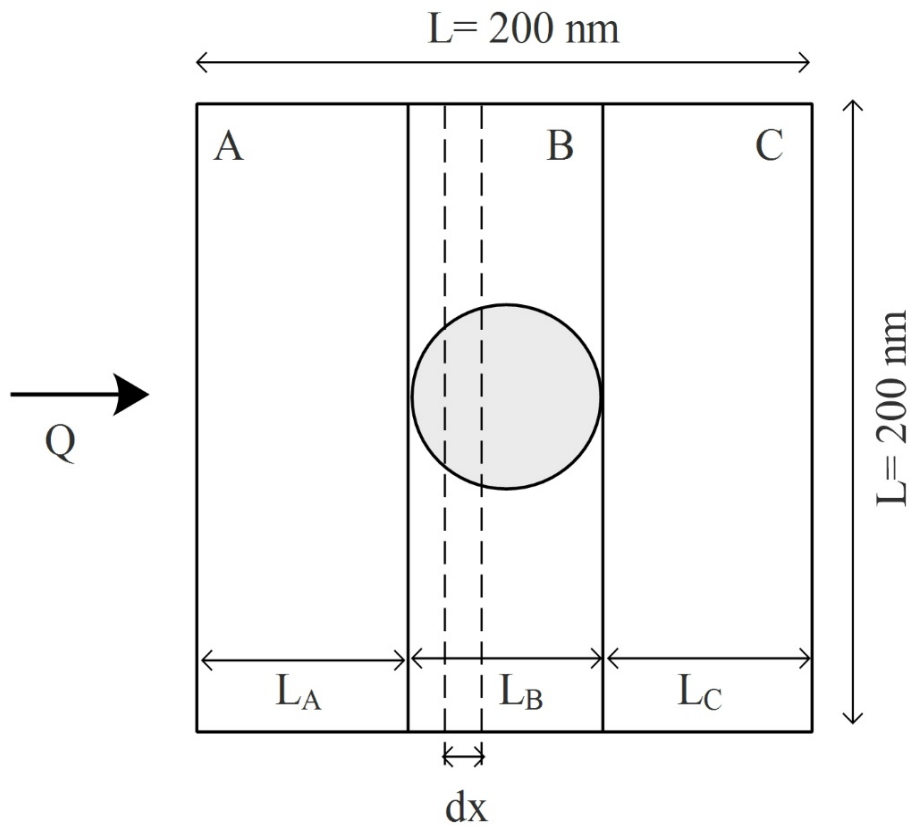


Figure 6.10 Heat transfer through different parts of the model

In part B total heat ( $Q$ ) divides into two parts. Heat  $Q_1$  flows through material 1 (host) and  $Q_2$  through material 2 (filler). Taking a thin elemental piece of length  $dx$  and



applying Fourier's law of heat conduction, thermal conductivity  $k_B$  is written as equation 6.10.

$$k_B = \frac{Q_1 + Q_2}{A \left( \frac{\Delta T}{dx} \right)} \quad (6.10)$$

$$k_B = \frac{Q_1}{A \left( \frac{\Delta T}{dx} \right)} + \frac{Q_2}{A \left( \frac{\Delta T}{dx} \right)} \quad (6.11)$$

Using equation 6.9,  $k_B$  can be written as:

$$k_B = \frac{k_1 A_1}{A} + \frac{k_2 A_2}{A} \quad (6.12)$$

Where,  $A_1, A_2$  are cross section area of cube in part B and sphere in part B respectively.

Effective thermal conductivity of entire region B is given by:

$$k_B = \int_{L_B} \frac{\left( \frac{k_1 A_1}{A} + \frac{k_2 A_2}{A} \right) dx}{L_B} \quad (6.13)$$

$$k_B = \frac{k_1 V_1 + k_2 V_2}{L_B A} \quad (6.14)$$

Where,  $V_1, V_2$  in part B represents the volume of material 1 and material 2 respectively.

For illustration purposes, the lengths of parts A, B, and C are set to  $L_A=75$  nm,  $L_B=50$  nm, and  $L_C=75$  nm, respectively, while the thermal conductivity values of the host and spherical filler material are set to 5 W/K.m and 10 W/K.m, respectively. For these numerical values, equation 6.14 calculates an effective thermal conductivity of 5.163624 W/K.m for portion B.

Thermal resistance of part A, part B and part C are given by:

$$R_A = \frac{L_A}{A \cdot K_A} \quad (6.15)$$

$$R_B = \frac{L_B}{A \cdot K_B} \quad (6.16)$$

$$R_C = \frac{L_C}{A \cdot K_C} \quad (6.17)$$

$R_A$ ,  $R_B$  and  $R_C$  are calculated as  $3.75 \times 10^{-4}$  K/W,  $2.42 \times 10^{-4}$  K/W and  $3.75 \times 10^{-4}$  K/W respectively. Equivalent thermal resistance of series region i.e. A, B, and C is given by:

$$R_{\text{equivalent}} = R_A + R_B + R_C \quad (6.18)$$

Computed equivalent thermal resistance of the composites is given by  $9.92207 \times 10^{-4}$  K/W.

Hence, effective thermal conductivity of the composites structure is given by:

$$k_{\text{effective}} = \frac{L}{A \cdot R_{\text{equivalent}}} \quad (6.19)$$

By substituting specified numerical values in equation 6.19, the effective thermal conductivity of composites is determined to be 5.039 W/K.m. As can be seen, the analytical solution deviates from the numerical solution by only 0.16 %. Thus, the modeling technique is justified in terms of physics, domain properties, and boundary conditions, as the numerical solution obtained matches the analytical solution quite well.

### **6.3.1.2.6 Estimating thermal conductivity of interphase in nanocomposites**

Numerical modeling approach to estimate effective thermal conductivity in composites is validated in the preceding section. This part intends to estimate the effective thermal conductivity of nanocomposites model depicted in Figure 6.2. The thermal conductivity of interphase is estimated using the methodology described in section 5.4. The following steps are followed to estimate the thermal conductivity of interphase:

Step 1-Record experimental thermal conductivity values for pure epoxy and nanocomposites.

Step 2-Import the model created in COMSOL Multiphysics. Assign material properties, describe the model's physics, and apply appropriate boundary conditions.

Step 3-Set the simulated thermal conductivity of nanocomposite to zero as an initial trial value. Specify a convergence tolerance value of 0.001. Assign a value of 0 as the initial mean, a value of 30 as the upbound, and a value of 0.001 as the lowbound.

Step 4-Compare measured thermal conductivity of nanocomposites to that computed using a numerical model. If this difference is more than the convergence tolerance limit, go to the next step. If the difference is less than the convergence tolerance, store the interphase's thermal conductivity value and exit the program.

Step 5-Calculate the mean value of upbound and low bound. Assign this mean value to interphase thermal conductivity.

Step 6-Calculate the total heat flux and temperature gradient using the numerical model. Determine the thermal conductivity of nanocomposite using total heat flux magnitude and temperature gradient. This nanocomposite thermal conductivity value should be stored.

Step 7-The computed value of the effective thermal conductivity of the nanocomposites is compared to the measured value. If the computed value exceeds the measured value, then assign upbound as the mean value. If the computed value is lower than the measured value, then a low bound is used as the mean.

Step 8-Return to step 4 and repeat until convergence is achieved.

For sake of clarity, this proposed algorithm is also depicted using a flow chart in Figure 6.11.

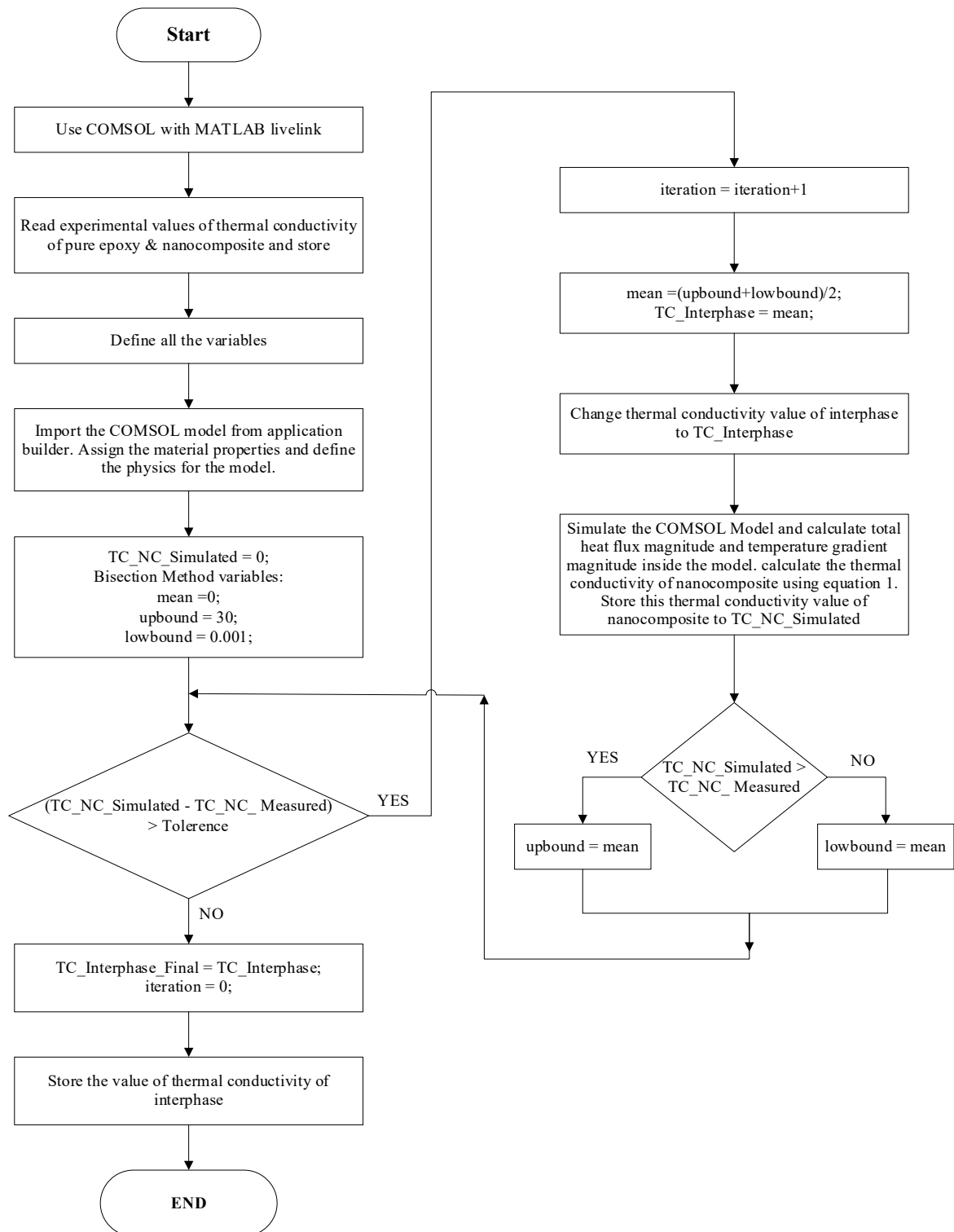


Figure 6.11 Flowchart to estimate the thermal conductivity of the interphase

## 6.4 RESULT AND DISCUSSION

The thermal conductivity of alumina particles as specified by the manufacturer is 30 W/K.m, and the measured thermal conductivity of neat epoxy samples is 0.16 W/K.m. This shows that the epoxy resin (a thermoset polymer) possesses significantly lower thermal conductivity than alumina. XRD spectra of epoxy and alumina nanoparticles are shown in Figure 4.3a and 4.3b, respectively. The XRD pattern clearly indicates the amorphous and crystalline nature of epoxy and alumina, respectively. One of the main reasons for the lower thermal conductivity of epoxy resin is its high degree of amorphousness. Besides being amorphous, epoxy resin exhibits low thermal conductivity due to its low atomic density and higher mismatch in its molecular thermal vibrations.[105] The XRD pattern of epoxy alumina nanocomposites is shown in Figure 4.3c explicitly indicates the presence of alumina particles in composite samples.

The effect of nanofiller inclusion on the thermal conductivity of epoxy is estimated using the numerical model described earlier. To begin, the numerical model treats nanocomposites as a two-phase system. The computed thermal conductivity is then compared with the measured thermal conductivity. The bar chart in Figure 6.12 shows the measured and numerically estimated effective thermal conductivity of nanocomposite samples. The calculated thermal conductivity of nanocomposites is significantly lower than the measured value. Thus, considering a nanocomposite sample as a two-phase system is unacceptable, particularly when nanocomposites are synthesized using surface-treated nanoparticles. Chapter 4 presented a detailed analysis to demonstrate how the interaction of a surface-treated filler and polymer matrix would eventually result in the formation of interphase. The algorithm discussed in the previous section predicts interphase thermal conductivity of 0.351 W/K.m.

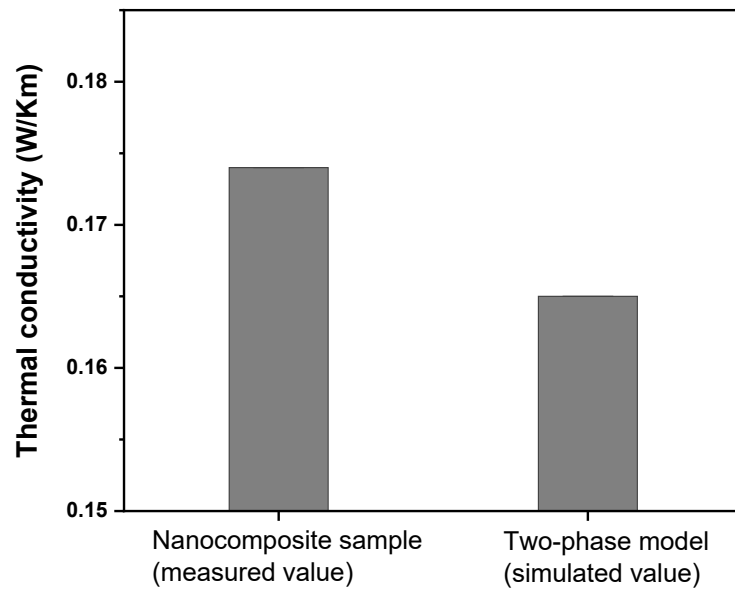


Figure 6.12 Thermal conductivity of nanocomposite sample (measured value) and simulated value for a two-phase model

In order to validate the estimated thermal conductivity of interphase, a numerical model is built with a nano alumina content of 2 vol.%. The effective thermal conductivity of nanocomposites (with filler content of 2 vol.%) is determined by ascribing known material properties to each of the three phases (i.e., base polymer, filler, and interphase). Epoxy resin, alumina, and interphase have thermal conductivity of 0.16, 30, and 0.351 W/K.m, respectively. The numerical model predicts that the effective thermal conductivity of nanocomposites is 0.191 W/K.m, which is consistent with experimentally determined thermal conductivity.

Furthermore, for a three-phase system, the effective thermal conductivity of composites should lie within the upper and lower Wiener bounds[106]. The upper and lower wiener bounds are given by (6.20) and (6.21).

$$k_{upper} = \phi_p \cdot k_p + \phi_i \cdot k_i + (1 - \phi_p - \phi_i) \cdot k_m \quad (6.20)$$

$$k_{lower} = \left[ \frac{\phi_p}{k_p} + \frac{\phi_i}{k_i} + \frac{(1-\phi_p-\phi_i)}{k_m} \right]^{-1} \quad (6.21)$$

where,

$k_{upper}$  - Upper wiener bound

$k_{lower}$  - Lower wiener bound

$\phi_p$  - Volume fraction of filler particles

$\phi_i$  - Volume fraction of interphase

$k_p$  - Thermal conductivity of filler particles

$k_i$  - Thermal conductivity of interphase

$k_m$  - Thermal conductivity of the matrix

For a nanocomposite sample with a filler content of 1 vol.%,  $k_{upper}$  and  $k_{lower}$  are 0.471 W/K.m and 0.168 W/K.m, respectively. The effective thermal conductivity of epoxy alumina nanocomposites predicted using the numerical model is 0.174 W/K.m, and this value lies within the upper and lower Wiener bounds. Similarly, effective thermal conductivity estimated by the proposed numerical model for nanocomposites (containing 2 vol.% of nano alumina) is within Wiener bounds. Thus, each of the studies described above verifies the accuracy of the numerical model. Interphase thermal conductivity is calculated to be substantially greater than the thermal conductivity of the neat polymer. High thermal conductivity of interphase may be attributed to the polymer chain's alignment at filler matrix interfaces. Andritsch[107] proposed a polymer chain alignment model and explained how aligned chains might contribute to a nanocomposites sample's effective permittivity. Similarly, few other researchers[70], [72], [108]–[113] have published on the impact of chain alignment on the thermal conductivity of polymers. Heat transfer in insulating polymers is thought to be primarily facilitated by phonon transport. As shown in Figure 6.13, polymers' irregular crystal structure results in the scattering of thermal energy carriers (phonons). Polymeric materials with increased phonon scattering have low thermal conductivity.



Aligned polymer chains minimize interfacial resistance, thus facilitating the phonon transport between filler and base epoxy, and vice versa. The schematic in Figure 6.14 illustrates how aligned polymer chains at the interfaces can boost phonon transport, resulting in an increase in interphase thermal conductivity. This means that the structural modification at the interface ultimately manifests as an increase in the thermal conductivity of nanocomposites.

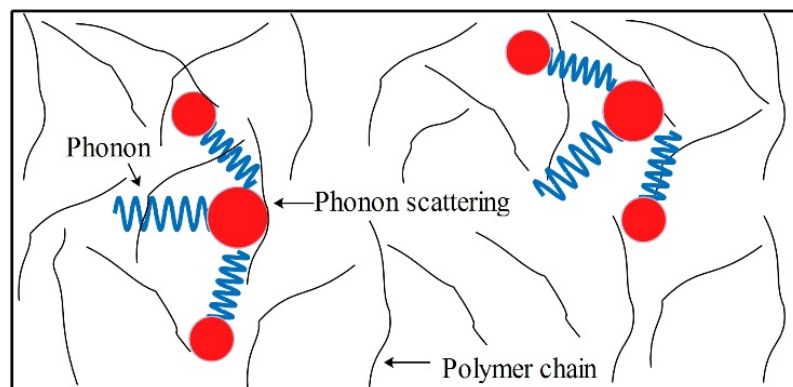


Figure 6.13 Phonon scattering phenomena in a polymer.

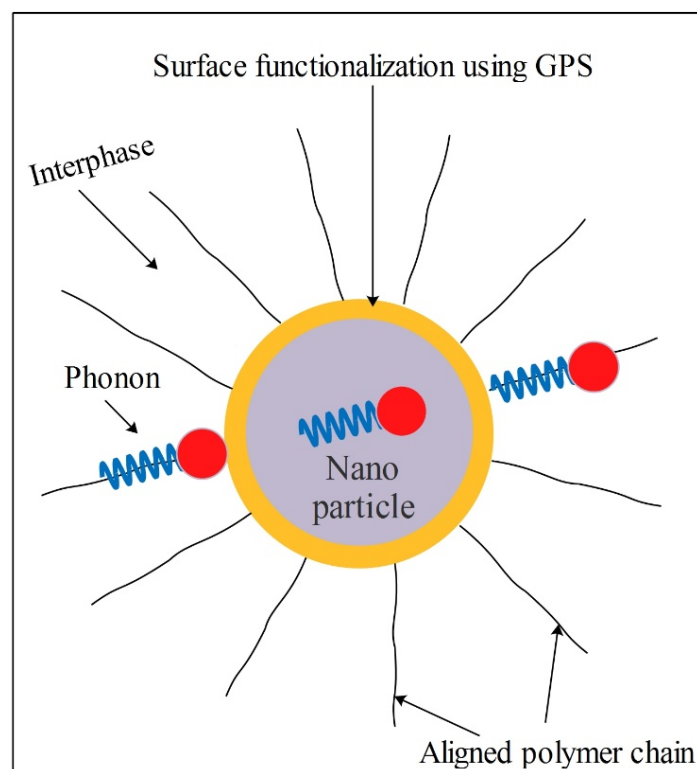


Figure 6.14 Phonon transport phenomena through aligned polymer chains in interphase.

**6.5 SUMMARY**

A computational approach for estimating the electrical and thermal conductivity of interphase in epoxy alumina nanocomposites is developed. Based on experimental data and numerical modeling, a complete analysis reveals that the thermal conductivity of interphase in epoxy alumina nanocomposites is much higher than that of neat epoxy. The interphase's electrical conductivity (dc) was observed to be lower than that of neat epoxy. The aligned polymer chain at filler matrix interfaces may be responsible for the high thermal conductivity of the interphase. The alignment of the polymer chain lowers phonon scattering and hence improves heat transmission efficiency. Furthermore, filler matrix interaction at the interface may promote crystallinity, which reduces electrical conductivity. As a result, nanocomposites made with surface-treated nanofillers are successful in increasing thermal conductivity while decreasing electrical conductivity. This quantitative examination of interphase thermal and electrical conductivity will aid in evaluating the performance of nanocomposites with varying filler concentrations, filler morphologies, and orientation. This will provide useful information and new insights for the thermal design of a complicated system using nanocomposites. Using quantitative data on interphase from the current work, the following chapter analyses the optimal filler concentrations for improved electro-thermal properties.